# Airway Inspector: an Open Source Application for Lung Morphometry

Raúl San José Estépar[1], George G. Washko[2], Edwin K. Silverman[2,3], John J. Reilly[2], Ron Kikinis[1], and Carl-Fredrik Westin[1]

[1] Surgical Planning Lab, Brigham and Women's Hospital, Boston, MA
{rjosest,westin,kikinis}@bwh.harvard.edu
[2] Pulmonary and Critical Care Division, Brigham and Women's Hospital, Boston, MA {gwashko,jreilly}@partners.org
[3] Channing Laboratory, Brigham and Women's Hospital, Boston, MA
reeks@channing.harvard.edu *

**Abstract.** Quantitative analysis of computed tomographic (CT) images of the lungs is becoming increasingly useful in the medical management of subjects with Chronic Obstructive Pulmonary Disease (COPD) and other lung diseases. Airway Inspector is an open source initiative based on 3D Slicer for the morphometric analysis of airway trees and lung parenchyma to foster the quantitative needs to carry out image-based lung disease studies. Airway Inspector allows the user to navigate an airway tree and provide airway morphometric measurements at every points. The airway wall extraction can be done by several methods, namely, traditional methods like Full-Width at a Half Max (FWHM) and Zero Crossing of the Second Order Derivative (ZCSEC), and a new breed of methods based on phase congruency. Airway Inspector can also perform quantitative analysis of parenchyma diseases by means of histogram analysis of the lung parenchyma CT density.

## 1 Introduction

Recent investigations using quantitative image analysis of multislice CT (MSCT) data sets have provided new insights into the characterization of both emphysema and airway disease. For example, measurements of airway wall thickness on CT images are predictive of lung function; thicker airway walls tend to be found in subjects with reduced airflow [16]. This increased interest in using CT scans for the characterization of lung disease has unveiled the need for a software platform that can be used to implement reliable methods for lung CT analysis. Given the evolving nature of the field, an open platform is an optimal way to test different approaches and perform the necessary validation that is needed before those methods can be used in research networks and clinical trials.

Airway Inspector (www.airwayinspector.org) is a open source software platform for the morphometric analysis of lung CT images based on 3D Slicer. 3D

* This work has been funded by grants R01 HL68926, P41-RR13218, R01 HL075478 and P01 HL083069

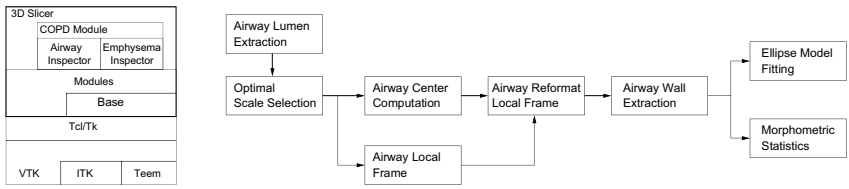


**Fig. 1.** (a) Airway Inspector and 3D Slicer software components and dependencies. (b) Computational components of Airway Inspector.

Slicer (www.slicer.org) is a free open source platform for medical image visualization and computing developed at the Brigham and Women's Hospital. 3D Slicer is available under a BSD-style license that has been also adopted by Airway Inspector. 3D Slicer has a modular architecture that allow the developers to extend its capabilities by adding new modules. The modules are mostly written in C++ and Tcl/Tk. While C++ is used to implement the main processing elements, Tcl/Tk is used for GUI design, interfacing and quick prototyping by means of wrappers to the methods implemented in C++. The main libraries that 3D Slicer depends on are the Visualization Toolkit (VTK) [19] and the Insight Toolkit (ITK) [23] for image visualization and image processing respectively. Additionally, 3D Slicer also depends on Teem [8], a multipurpose collection of libraries for representing, processing, and visualizing scientific multidimensional raster data. A diagram showing the dependencies of Airway Inspector is shown in Fig. 1a.

Airway Inspector is a component of the COPD module; a module for the analysis of both parenchyma and airway diseases. As such, the module implements different quantitative methods for the assessment of emphysema and the assessment of airway wall remodeling by means of Airway Inspector.

## 2 Airway Inspector: Computational Components

The main computational components of Airway Inspector are shown in Fig. 1b.

### 2.1 Airway Lumen Extraction

The entry point to Airway Inspector is a point inside the airway lumen under interrogation. This point can be either manually selected by an user or it can be automatically extracted by means of the segmentation of the airway lumen tree and the extraction of the centerline. For the automatic segmentation of the airway tree, Airway Inspector currently relies on the *Editor* module capabilities provided by 3D Slicer. The *Editor* module allows the user to perform a region growing process from a seed point placed, for example, in the trachea. After the segmentation of the airway tree, the COPD module provides a method to extract the centerline [2].

### 2.2 Continuous data reconstruction

An ubiquitous functionality across different computation components is the need of continuous data reconstruction, data interpolation and differentiation operations (first order and second order derivatives). To that end, Airway Inspector relies on Teem. The library inside Teem that takes care of the reconstruction is gage. Gage is an interface for continuous data reconstruction from sampled data. Gage implements different interpolation kernels; among them, the traditional cubic B-spline [13, 10] is used to compute intensity data at a continuous location and the corresponding gradient vector and Hessian matrix at that location.

### 2.3 Automatic scale selection

When querying the derivative operator at a given point, a critical factor is the scale at which those derivatives should be extracted. Based on the seminal work of Eberly [4], airways can be seen as valley lines of intensity. The Hessian matrix capture second-derivative information that can distinguishes ridges and valley lines, saddles, valley surfaces and ridge surfaces, and spheres. For a valley line the Hessian matrix, at the right scale, is characterized by two large positive eigenvalues ($\lambda_1 >> 0$, $\lambda_2 >> 0$) and one small negative eigenvalue ($\lambda_3 < 0$). At the valley point, the gradient should be orthogonal to the eigenvectors associated to the positive eigenvalues.

Although a formal scale-space analysis is not carried out [11], the automatic scale selection process seeks the optimal reconstruction kernel support, $\sigma_{opt}$, such as the following functional of the eigenvalues is maximized

$$\sigma_{opt} = \underset{\sigma}{argmax} \quad \frac{\lambda_1(\sigma) + \lambda_2(\sigma)}{2} - |\lambda_3(\sigma)| \tag{1}$$

where $\lambda_i$ is the Hessian eigenvalue associated to the eigenvector $\mathbf{e}_i$. This optimal kernel size computed at the selected airway point is used hereon.

### 2.4 Airway Centering

The first step after a point inside the airway of interest has been chosen is to perform a centering of the point. The center is defined as the centroid, $\mathbf{x}_c$ of the luminal area. The luminal region is defined in the axial plane by means of a thresholding. The threshold is automatically defined as the mean value of the minimum and the maximum intensity values found in two rays in the form of a cross casted from the selected point.

After the centroid is located, a second step refines that location using the properties of the Hessian matrix. The centroid location, $\mathbf{x}_c$, is optimized using a gradient descent in the direction of the projected gradient, $\mathbf{g}_p(\mathbf{x})$, given by

$$\mathbf{g}_p(\mathbf{x}) = (\mathbf{I} - \mathbf{e}_3\mathbf{e}_3^T)\nabla I(\mathbf{x}). \tag{2}$$

The result of the optimization process is the final airway luminal center location, $\mathbf{x}_l$. The Hessian eigenvectors are computed at the optimal scale, $\sigma_{opt}$.

When the slice thickness is larger than the in-plane resolution, a full volumetric approach is not reliable, at least in the slice direction. Then, $\mathbf{x}_l$ is only computed in the axial plane by descending in the in-plane 2D gradient direction.

### 2.5 Airway Local Frame

The Hessian matrix at the optimal scale, $\sigma_{opt}$, can be used to estimate the direction of the airway longitudinal axis and define a local reference frame, if not already available through the centerline extraction process. The longitudinal airway axis, $\mathbf{a}_z$ is given by the eigenvector associated to the most negative eigenvalue at the airway center location, $\mathbf{x}_l$, such as $\mathbf{a}_z = \mathbf{e}_3(\mathbf{x}_l)$. A local frame for the airway locations, $\mathbf{x}_l$, is defined as the vectors $\mathbf{a}_x$ and $\mathbf{a}_y$ that form an orthonormal basis with $\mathbf{a}_z$ and at the same time are maximally aligned with the scan axial directions.

Based on the airway local frame and center, a 2D slice containing the whole airway is interpolated for further processing. Airway Inspector allows the user to perform the interpolation in two ways; either in the oblique plane or the native axial plane, if the slice thickness is not suitable for a reliable interpolation in the z-direction. The oblique plane is defined as the plane whose normal is given by the airway longitudinal axis, $\mathbf{a}_z$. The field of view (FOV) of the reformatted airway plane is equal to 25.6 mm, although this value can be modified accordingly to accommodate larger airways.

### 2.6 Airway wall extraction

The airway wall is defined by casting rays at regular angular increments from the center location, $\mathbf{x}_l$. For each ray, the intensity profile of the 2D reformatted slicer is interpolated at 0.05 mm. Each ray, $A_\rho(r)$, is a profile that comprises a lumen section, a wall section and a parenchyma section. Airway Inspector currently implements four methods for the definition of the inner and outer wall boundaries. In section 3, we will elaborate on these methods.

The result of the wall extraction process is the inner and outer radial locations, $r_i(\rho)$ and $r_o(\rho)$ respectively, at the polar angle $\rho$. The airway wall boundaries in the local frame defined by the axes $\mathbf{a}_x$ and $\mathbf{a}_y$ are given by point set $x_{i/o} = r_{i/o}(\rho)cos(\rho)$ and $y_{i/o} = r_{i/o}(\rho)sin(\rho)$ in Cartesian coordinates. The current implementation uses 128 rays equally distributed in the interval $[0, 2\pi)$ radians.

### 2.7 Ellipse Fitting

The airway extraction methods are based on a ideal circular model for the airway. Due to adjacent vessels and other image artifacts, the airway detection can be challenging and airway wall points can be noisy. To yield a more robust measurement, a ellipse model is fitted to the set of points $\{x_{i/o}, y_{i/o}\}$ using the method proposed in [7, 5]. Both the native ray-based measurements as well as the ellipse model parameters are available for the user.

### 2.8 Airway labeling

Currently the airways are label in four categories: right/left upper/lower lobe, based on the relative location of the airway center $\mathbf{x}_l$ with respect to the CT volume center. The user can redefine this assignment if it is not correct.

### 2.9 Morphometric statistics

From the polar parametrization of the inner and outer wall, several morphometric quantities are computed for each selected airway. For each quantity, mean, standard deviation, maximum and minimum values are reported. The morphometric quantities that Airway Inspector currently reports are:

- Inner, outer radius and wall thickness.
- Inner and outer perimeter: the perimeter is computed as a piecewise approximation based on the data points
- Inner, outer and wall area: the area is computed as a piecewise approximation of the area for each ray sector.
- Inner and outer ellipse parameters: the parameters of the ellipse fitting process are the length of the major and minor axes and the angle that the major axis with respect to $\mathbf{a}_x$.
- X-ray attenuation: airway inspector provides different metrics for the measured intensity inside the wall. Those metrics include the mean wall intensity inside the wall, peak wall intensity (maximum X-ray attenuation inside the airway wall for each ray) and the inner and outer luminal intensities (X-ray attenuation at the location of the inner and outer wall respectively).

## 3 Airway wall morphology

Airway Inspector currently implements four different methods for the extraction of the airway wall boundaries and it is poised to be an extensible platform where new airway wall extraction methods can be implemented and compared against is peers. Methods for the estimation of the airway wall can be divided in two categories: parametric [17, 3, 20, 22] and non-parametric [1, 18]. The former methods rely on an estimation of the scanner point spread function (PSF), therefore they can provide measurements beyond the limit imposed by the pixel resolution. The latter do not use any knowledge about the scanner PSF, therefore their measures are more limited in range. Airway Inspector currently only implements non-parametric methods given that they do not imply any knowledge about the acquisition process. The implemented methods can be divided in two categories: traditional methods and new methods based on phase congruency.

### 3.1 Traditional Methods

**FWHM.** FWHM defines the wall boundaries at the location where the intensity profile is half the intensity between the peak intensity inside the wall and the intensity of the inner/outer valley areas. Let $r_{max}$ be the location of the maximum of the intensity profile $A_\rho(r)$ and $r^i_{min}$ and $r^o_{min}$ be the locations of the minimum intensity that are observed in the inner and outer walls, respectively. Formally, the FWHM is given by

$$r_i(\rho) = A_\rho^{-1}\left(\frac{A_\rho(r_{max}) - A_{CT}(r^i_{min})}{2}\right); \quad r_o(\rho) = A_\rho^{-1}\left(\frac{A_\rho(r_{max}) - A_{CT}(r^o_{min})}{2}\right), \tag{3}$$

where $A_\rho^{-1}$ is the inverse function of $A_\rho$ that maps intensity values into radial locations. As seen from eq. (3), a robust and accurate determination of the wall location based on the FWHM principle relies on a proper estimation of the peak and valley locations (also known as *extrema* points): $\rho_{max}$, $\rho^i_{min}$ and $\rho^o_{min}$. These values can be worked out by means of the first order derivative.

$$\frac{dA_\rho}{dr}(r_{max}) = 0; \quad \frac{dA_\rho}{dr}(r^i_{min}) = 0; \quad \text{and} \quad \frac{dA_\rho}{d\rho}(\rho^o_{min}) = 0. \tag{4}$$

Moreover, if we want to distinguish between the peak and the valley points, we can inspect the sign of the second order derivative, such that

$$\frac{d^2A_\rho}{dr}(r_{max}) < 0; \quad \frac{d^2A_\rho}{d\rho}(r^i_{min}) > 0; \quad \text{and} \quad \frac{d^2A_\rho}{dr}(r^o_{min}) > 0. \tag{5}$$

In summary, the first order derivative of the intensity profile is the main operator that allows for the computation of the wall location based on the FWHM principle. FWHM is quite sensitive to the selection of these locations and slight differences in implementation can change the results yielded by FWHM. Airway inspector uses gage to compute the needed derivatives along the ray direction and the Newtwon-Raphson method [24] for the computation of the roots of the first-order derivative.

**ZCSEC.** Based on the edge detection theory proposed by Marr and Hildreth [12], the location of a boundary is defined as the inflection point between the valley intensity and the peak intensity. This inflection point is located at the zeros of the second order derivative; thus, the airway wall locations can be formally defined as $\frac{d^2A_\rho}{dr^2}(r_i) = 0$ and $\frac{d^2A_\rho}{dr^2}(r_o) = 0$. The zero location of the second order derivatives are computed using Netwon-Raphsons method.

### 3.2 Phase Congruency Methods

Based on the work by Morrone et al. [14], edge locations are related to those locations where the local Fourier components of the intensity signal are maximally in phase [9]. This *in-phase* behavior has been denoted as phase congruency and it has been used by the computer vision community as a feature descriptor [15, 6]. Airway Inspector defines the airway wall boundaries as the locations of maximal phase congruency. Phase congruency can be computed either by means of multiple CT reconstruction kernels by effectively changing the CT modulation transfer function or by means of a computational approaches using a single reconstruction kernel. We have previously reported these methods for the computation of airway wall location and we have shown their superiority with respect to traditional methods [18].

**Single reconstructions.** Phase congruency can be estimated by analyzing the input signal with a bank of complex-value quadrature filters, $\mathbf{g}_n(x)$, $n = 0, \ldots, N-1$. The output of a quadrature filter is a complex-value signal whose

magnitude and argument represents the local energy and the local phase of the input signal respectively. The quadrature filter bank used in Airway Inspector is a log-Gabor family given by, in the Fourier domain,

$$G_n(\omega) = e^{-\frac{\log^2(\frac{\omega}{\omega_n})}{2log^2(\frac{\kappa}{\omega_n})}}, \tag{6}$$

where $\omega_n$ is the central frequency of the filter and $\kappa$ is related to the filter bandwidth. The filter bank is defined in Airway Inspector by three parameters that can be adjusted by the user: number of filters, $N$, the bandwidth of the filters, $B$ (in octaves), and a multiplication factor that defines the separation of the filters, $m_{\lambda_{min}}$. The central frequency for each filter in the bank is given by the series $\omega_n = \frac{2\pi}{m_\lambda^n \lambda_{min}}$ where $n$ is the $n$-th filter and $\lambda_{min}$ is the spatial wavelength of the highest frequency filter and has a nominal value of 4 samples.

After filtering the 1D intensity profiles with the bank of quadrature filters, Airway Inspector computes phase congruency as

$$\Psi_\theta(r) = \frac{\sqrt{\left(\sum_{n=0}^{N-1} \mathrm{Re}\left\{A(r) * \mathbf{g}_n(r)\right\}\right)^2 + \left(\sum_{n=0}^{N-1} \mathrm{Im}\left\{A(r) * \mathbf{g}_n(r)\right\}\right)^2}}{\sum_{n=0}^{N-1} \left\|A(r) * \mathbf{g}_n(r)\right\|} \times \tag{7}$$
$$max\left(cos(\bar{\phi}(x) - \theta), 0\right),$$

where $\theta$ depends on the feature type we want to extract by means of phase congruency. Based on the meaning of the local phase, for the detection of the inner wall interface $\theta = \pi/2$ and for a outer wall interface $\theta = \frac{3\pi}{2}$. Then, the inner and outer wall location are estimated by finding the location that maximizes $\Phi_{\pi/2}(x)$ and $\Phi_{3\pi/2}(x)$ respectively. $\bar{\phi}(x)$ is the energy weighted mean local phase and can be approximated by

$$\bar{\phi}(x) = \mathrm{atan2}\left(\sum_{n=0}^{N-1} \mathrm{Im}\left\{A(r) * \mathbf{g}_n(r)\right\}, \sum_{n=0}^{N-1} \mathrm{Re}\left\{A(r) * \mathbf{g}_n(r)\right\}\right), \tag{8}$$

where $atan2(\cdot,\cdot)$ is the four quadrant inverse tangent.

**Multiple reconstructions** When multiple CT reconstructions are available, maximal phase congruency is expressed as a common crossing point in the intensity profiles of the kernels [18]. If multiple kernels are available, Airway Inspector reformats the airway for each kernel and detects the common crossing point for each 1D ray as the median intersection point for all possible pairwise combinations of kernels. The median operator is used because it is a robust estimator. If we have $K$ kernels, the number of pairwise combinations is $M = \frac{K!}{2(K-2)!}$. Let $V$ be the set of all pairwise combinations and $V(i)$ the $i-th$ pair of the set. Let $Inter_i$ and $Inter_o$ be the intersection operator that computes the intersection point between two kernel profiles for the inner and outer walls, respectively. The inner and outer wall locations are then given by $\rho_{i/o} = \mathrm{median}\left(\bigcup_{i=1}^{M} Inter_{i/o}\{V(i)\}\right)$ respectively.

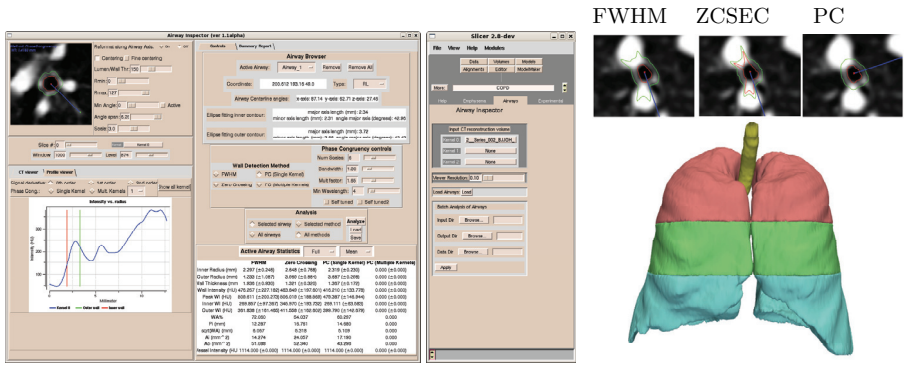


**Fig. 2.** (a) Airway Inspector GUI interface. (b) COPD module GUI. (c) Top- detected airway with FWHM, ZCSEC and phase congruency. Botton- Lung extraction.

## 4 Software functionalities

Figure 2a shows a snapshot of the current user interface for Airway Inspector. After the selection of several airway locations, the user can browse different airway locations and can probe the intensity profile by moving the mouse over the airway viewer. The airway wall is also plotted on the airway viewer for the method currently active. The panel below the airway viewer shows a plotting of the intensity profile, intensity derivatives, phase congruency responses ($\Phi_{\pi/2}(x)$ and $\Phi_{3\pi/2}(x)$) and the location of the estimated airway wall at the given ray for the selected method. In the left panel the user can control the analysis by selecting a detection method. The user can analyze either a given airway or all the loaded airways. The analysis can be run for a given wall detection method or all implemented methods. The results are reported in the lower left panel. A general statistical summary is shown as a separate tab on the left panel. Three airway viewer examples for each implemented detection method are shown in Fig. 2c. Phase congruency produces the most consistent results having the best performance in challenges areas like sections of the airway closed to vessels.

Additional features are the possibility of saving the current analysis in a Comma Separated Values (CSV) file format. This file can be later loaded into Airway Inspector and both the airway locations and the corresponding scan are automatically loaded for further analysis. A batch mechanism is in place (see Fig. 2b) that enables a automatic reanalysis of the data. The user can select the directories containing both the Airway Inspector files and the CT scans, and the software automatically loads every case, reanalyzes the data and saves the new analysis files into a directory.

Besides Airway Inspector, the COPD module integrate another package, Emphysema Inspector, for emphysema CT-based quantification based on histogram analysis. As part of this package, the lungs are automatically segmented into

three regions of equal volume, the trachea is extracted and the major vessels inside the parenchyma are also identified as shown in Fig 2c.

## 5 Conclusions

Airway Inspector is a Free Open Source software package for the morphometric analysis of airway trees. More information about the project, tutorials and source code can be found in www.airwayinspector.org. Although high-quality commercial software packages, like VIDA [21], exist, Airway Inspector is one of the first attempts to offer an open platform for the implementation of new airway morphometry methods that can foster the application of CT-based quantitative research. Airway Inspector is an evolving tool and some of the future features are the following:

- Implementation of a reliable method for automatic extraction of tubular structures in the lung: airway lumen and pulmonary vessels.
- Automatic filter bank design for phase congruency based on the prior knowledge of the structure size that is to measured.
- Automatic labeling of airway generations according to anatomical standards.
- Support for airway generation-based statistics.
- Group-wise registration of airway trees corresponding to a population to enable group statistical analysis.
- Porting to the next 3D Slicer generation (Slicer 3).
- Lobular segmentation.
- Integration with grid computing infrastructures to enable processing of large cohorts.

Further work is also needed to validate the airway extraction and wall detection methods across platforms. Both accuracy and precision are key components to study when designing a validation experiment. These kind of studies are very important for the adoption of computer-based CT morphometry of the lung in clinical research.

## References

1. I. Amirav, S. S. Kramer, M. M. Grunstein, and E. A. Hoffman. Assessment of methacholine-induced airway constriction by ultrafast high-resolution computed tomography. *J. Appl. Physiol.*, 75:2239–2250, 1993.
2. Sylvain Bouix, Kaleem Siddiqi, and Allen Tannenbaum. Flux driven automatic centerline extraction. *Medical Image Analysis*, 9(3):209–221, 2005.
3. Y. Cheng, Y. Sato, H. Tanaka, T. Nishii, N. Sugano, H. Nakamura, H. Yoshikawa, S. Wang, and S. Tamura. Accurate thickness measurement of two adjacent sheet structures in ct images. *IEICE Transactions on Information and Systems*, E90-D(1):271–282, 2007.
4. D Eberly, R Gardner, B Morse, and S Pizer. Ridges for image analysis. *Journal of Mathematical Imaging and Vision*, 4:351–371, 1994.
5. A. W. Fitzgibbon, M. Pilu, and R. B. Fischer. Direct least squares fitting of ellipses. In *Proc. of the 13th International Conference on Pattern Recognition*, pages 253–257, September 1996.

6. G. H. Granlund and H. Knutsson. *Signal Processing for Computer Vision*. Kluwer Academic Publishers, 1995. ISBN 0-7923-9530-1.
7. R. Halir and J. Flusser. Numerically stable direct least squares fitting of ellipses. In *Proc. of the 6th International Conference in Central Europe on Computer Graphics, Visualization and Interative Dgital Media (WSCG'98)*, volume 1, pages 125–132, October 1998.
8. Gordon L. Kindlmann. http://teem.sourceforge.net/.
9. Peter D. Kovesi. Image features from phase congruency. *Videre: Journal of Computer Vision Research*, 1(3):1–26, 1999.
10. Thomas M. Lehmann, Claudia Gönner, and Klaus Spitzer. Survery: Interpolation methods in medical image processing. *IEEE Trans. on Medical Imaging*, 18:1049–1063, 1999.
11. T Lindeberg. Edge detection and ridge detection with automatic scale selection. *International Journal of Computer Vision*, 30(2):77–116, November 1998.
12. D. Marr and E. Hildreth. Theory of the edge detection. *Proc. of the Royal Society of London B*, 207:187–217, 1980.
13. D Mitchell and A Netravali. Reconstruction filters in computer graphics. In *Proceedings ACM SIGGRAPH 1988*, pages 221–228, August 1988.
14. M. C. Morrone, D. C. Burr, J. Ross, and R. Owens. Mach bands are phase dependent. *Nature*, 324(1280):250–253, 1986.
15. M. C. Morrone and R. A. Owens. Feature detection from local energy. *Pattern Recognition Letters*, 6:303–313, 1987.
16. Y. Nakano and S. Muro et al. Computed tomographic measurements of airway dimensions and emphysema in smokers. *Am. J. Respir. Crit. Care Med.*, 162:1102–1108, 2000.
17. Joseph M. Reinhardt, Neil D. D'Souza, and Eric A. Hoffman. Accurate measurement of intra-thoracic airways. *IEEE Trans. Medical Imaging*, 16(6):820–827, Dec. 1997.
18. Raúl San José Estépar, George G. Washko, Edwin K. Silverman, John J. Reilly, Ron Kikinis, and Carl-Fredrik Westin. Accurate airway wall estimation using phase congruency. In *MICCAI'06*, volume 4191 of *Lecture Notes in Computer Science*, pages 125–134, October 2006.
19. W. Schroeder, K. Martin, and B. Lorensen. *The visualization toolkit: an object-oriented approach to 3D graphics*. Prentice Hall, 1998.
20. G. J. Streekstra, S. D. Strackee, M. Maas, R. ter Wee, and H. W. Venema. Model-based cartilage thickness measurement in the submillimeter range. *Medical Physics*, 34(9):3562–3570, 2007.
21. Juerg Tschirren, Eric A. Hoffman, Geoffrey McLennan, and Milan Sonka. Intrathoracic airway trees: Segmentation and airway morphology analysis from low-dose ct scans. *IEEE Trans. Medical Imaging*, 24(12):1529–1539, 2005.
22. Oliver Weinheimer, Tobias Achenbach, Carsten Bletz, Christoph Düber, Hans-Ulrich Kauczor, and Claus Peter Heussel. About objective 3-d analysis of airway geometry in computerized tomography. *IEEE Trans. on Medical Imaging*, 27(1):64–74, 2008.
23. Terry S. Yoo, editor. *Insight into Images Principles and Practice for Segmentation, Registration, and Image Analysis*. A K Peters, 2004.
24. Tjalling J. Ypma. Historical development of the newton-raphson method. *SIAM Review*, 37(4):531–551, 1995.